Observation of Equatorial Ionospheric Plasma Bubbles at Peninsular Malaysia by using MyRTKnet

Noor hijjah Mohd Yusof
Faculty of Electrical Engineering, Universiti Teknologi MARA,
40450 Shah Alam, Selangor, Malaysia
Muawizatain@yahoo.com

Abstract—**Depletion layer in Total Electron Content (TEC) in ionospheric layer is called plasma bubbles which usually occur during midnight. The research on observation of equatorial plasma bubbles (EPBs) ionospheric at peninsular Malaysia by using Malaysian Real Time Kinematic Global Positioning System Network (MyRTKnet) can be observed by ionosonde, radar, satellite, Global Positioning System (GPS)-receiver and being measured by using MyRTKnet. In this project, we will focus on data taken by GPS receiver only. This determination is made for satellites in Peninsular Malaysia in the September period of 2007. But only satellites at Universiti Utara Malaysia (UUMK) and Sungai Petani (SGPT) will be considered in this research. The important parameter in this project is TEC which is the value of TEC change rate; ∆TEC is taken within the period of every 15 seconds in order to detect Plasma Bubble. TEC is extracted using GPS receiver which in RINEX format that supplied by JUPEM (Department Of Survey and Mapping Malaysia) and taken from receiver station located at UUMK and SGPT. The value of ∆TEC is compared base on the dropness of TEC value within the scale. It is shown that most equatorial plasma-bubble events commence at 18:00 UT on 6th September 2007 for PRN 26, and may last for less than 60 min**.

Keywords— **Malaysian Real Time Kinematic Global Positioning System Network (myRTKnet), Total Electron Content (TEC), Receiver Independent Exchange Format (RINEX), Pseudorandom Number (PRN)**

1.0 INTRODUCTION

There are many disturbance in Ionosphere such as scintillation, travel ionosphere disturbance (TID), Plasma bubble etc. Plasma density depletion region which appears in the equatorial ionosphere is generated in the bottom side of the F region after the sunset of the ionosphere through plasma instability [1]. Accompanying electron density irregularities are formed in the post-sunset period at low magnetic latitudes is inherently unstable due to the gravitational Rayleigh-Taylor (RT) instability processes operating on the steep upward gradient in the bottom side F-region [2].

When the F-layer has risen to an altitude where the ion-neutral collision frequency is small, the local RT instability becomes susceptible to triggering and the condition is favorable for the development of irregularities. Earlier studies of the effects of geomagnetic storms on the development or inhibition of ionospheric irregularities have shown that there is a general consensus that magnetic activity tends to suppress the generations of spread-F or plasma bubbles in the pre-midnight period, whereas the possibility of observing spread-F or plasma bubbles during the post midnight period increases with magnetic activity[2].

However, as Palmroth et al. (2000) suggested, knowing the effects that the satellite cannot continuously position when the Dynamics Explorer (DE) 2 observed a plasma bubble the bubble probably had been generated a few hours before it was observed by the satellite.

In this research only data from GPS-receiver will be taken. GPS receiver networks, which provide global and continuous data, are powerful tools to investigate the occurrence rate of plasma bubble in detail because of complicated behavior of occurrence which have various temporal and spatial variations make it difficult to understand. Severe radio signal disruptions occur when the irregularities propagate into the topside ionosphere as density depletions called equatorial plasma bubbles (EPBs).

1.1 IONOSPHERIC LAYERS

The ionosphere is the uppermost part of the atmosphere where free electrons occurred in sufficient density to have an appreciable influence on the propagation of radio frequency electromagnetic waves to distant places on the Earth [3]. The ionospheric region are divided into three major layers which is each of the layer have different approximate height ranges; D-Layer (50 – 90 km), E-Layer (85 – 140 km) and F-Layer (140 – 1000 km) [4].

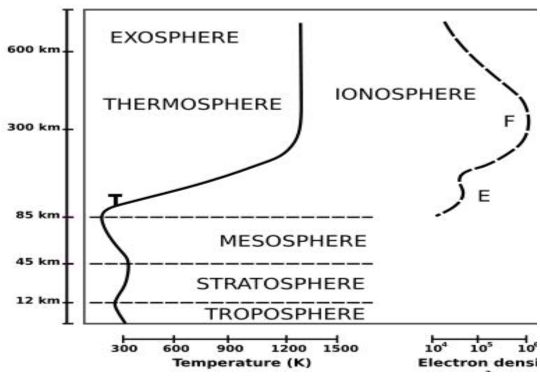

Fig. 1. Relationship of the atmosphere and ionosphere

The most important region is going to study here is F-Layer because the irregularities initially form in the bottom side of the F layer through a process referred to as a generalized Rayleigh -Taylor (R-T) Instability causing the greatest effect compared to the other layers on GPS received signal. During a plasma bubble, the ionosphere's F2 layer will become unstable, fragment, and may even disappear [5]. In this region the total electron content will occurred in the highest density with the nominal value 10^{16} to 10^{19} with minimum and maximum occurring at midnight and mid-afternoon [6] approximately as illustrates in figure (3).

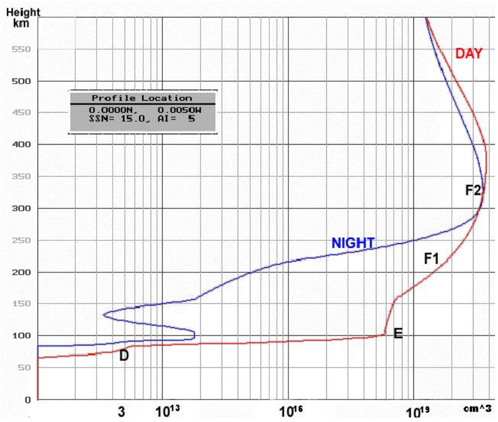

Fig. 2. Illustration of Total Electron Content in ionosphere at night and day.

1.2 TOTAL ELECTRON CONTENT (TEC)

TEC can be measured by using either GPS receivers or ionosonde. In this project, TEC will be measured by using GPS receivers. If a regional network of ground-based GPS receivers is used, then a map of TEC above the region can be constructed. The TEC normally varies smoothly from day to night as Earth's dayside atmosphere is ionized by the Sun's extreme ultraviolet radiation, while the night side ionosphere electron content is reduced by chemical recombination [7].

GPS satellites transmit electromagnetic waves for positioning on two frequencies: L1 (1.57542 GHz) and L2 (1.2276 GHz). The velocity of an electromagnetic wave at the GHz band is frequency dependent in the ionosphere. This enables us to extract the ionospheric TEC along the line of sight, satellite-receiver [8].

A. Ionospheric Delay and TEC

The ionosphere has a refractive index at radio frequencies which is different from unity and can affect GPS signals in a number of ways as they pass from satellite to ground (Klobuchar, 1996; Wanninger, 1993; Coco, 1991) [9].

This affect is the addition of ionospheric delay to GPS signals, thereby introducing an external bias source to pseudorange and carrier phase observations which is difficult to correct in single frequency receivers. However, dual frequency receivers are able to exploit the physics of the ionosphere as a dispersive medium in which the refractive index is a function of frequency, and introduce corrections which remove these effects, at least to a fist order [10].

The ionospheric time delay at the L1 carrier frequency f_1 is given by (Klobuchar,1996)

$$t_1 = 40.3 * \frac{(TEC)}{(cf_1^{\,2})} \tag{1}$$

where c is the speed of light in free space. A dual frequency receiver measures the difference in delay between the two frequencies, $\Delta t = t_2 - t_1$, given by

$$\Delta t = \left(\frac{40.3}{c}\right)\frac{(TEC)}{\left[\left(\frac{1}{f_2^{\,2}}\right)-\left(\frac{1}{f_1^{\,2}}\right)\right]} \tag{2}$$

which can be rewritten in the form

$$t_1 = \Delta t \times \left[\frac{f_2^{\,2}}{(f_1^{\,2} - f_2^{\,2})}\right] \tag{3}$$

where the delay t_1 can be regarded as the measured pseudorange at the L1 frequency. Rearrangement further of above equations will permit simple derivation of TEC, providing that all other sources of delay bias have fist been removed.

B. Calculation of Slant and Vertical TEC

Slant TEC is a measure of the total electron content of the ionosphere along the ray path from the satellite to the receiver, represented in Figure (6) as the quantity *Ts*. Vertical TEC, Tv enables TEC to be mapped across the surface of the earth [11].

The receiver (known as a ‘codeless’ receiver because it does not require knowledge of the C/A or P pseudorandom noise codes), by cross correlating the L1 and L2 modulated carrier signals, obtains the time delay of the P code and the carrier phase difference. These are used to calculate the pseudorange and differential carrier phase respectively, and hence the slant code TEC and slant phase TEC respectively [10].

The absolute TEC, from equation (6) can be calculated using GPS signal.

$$TEC = \frac{\Delta p.c}{40.3}\left(\frac{f_1^2 f_2^2}{f_1^2 - f_2^2}\right) \tag{4}$$

Where $\Delta\rho$ is the difference between time delays measured by the L1 and L2, C is the light velocity (m/s), f1 (1575.42 MHz) is the frequency of the L1 wave and f2 (1227.6 MHz) is the second frequency of the L2 wave.

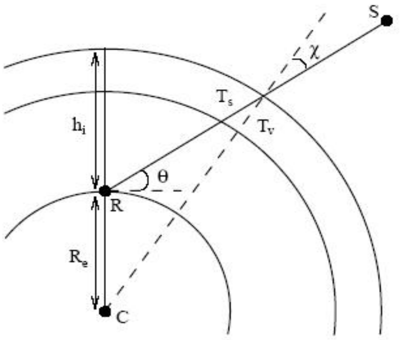

Fig.3. Geometry of Satellite-Receiver Link [10]

The slant total electron content, Ts or TECs, along ray path ,*l* between a GPS satellite, Tx, and a ground-based receiver, Rx, can be written as in equation (5) and (6) [12]:

$$TECs = \int_{Rx}^{Tx} N dl = \frac{f^2}{40.3}\int_{Rx}^{Tx}\left(n^{-1} - 1\right) dl \tag{5}$$

$$= \frac{f^2}{40.3}\int_{Rx}^{Tx}\left[\left(\sqrt{(1 - \frac{f_N^2}{f^2})}\right)^{-1} - 1\right] dl \tag{6}$$

Where N is the electron density in el/m^3, n denotes the refractive index, and f and f_N represent radio wave and plasma frequency in Hz, respectively. The *l*-axis stands for the receiver-to-satellite direction.

The slant TEC, TECs also can be written as in equation (7):

$$TECs = \frac{1}{40.3}\left(\frac{f_1^2 f_2^2}{f_1^2 - f_2^2}\right)\left(P_2 - P_1\right) \tag{7}$$

Equation (8) is to convert slant TEC (TECs) to vertical TEC (TECv).

$$TECv = TECs\ (\cos\ \chi') \tag{8}$$

Where TECs is the value of slant TEC, χ' is the difference between 90° and zenith angle (90°-χ).

In this TEC research, to get more precise mapping, the Modified-Single Layer Model, M-SLM is use as define in equation (9)

$$\sin\ \chi' = \frac{\mathrm{Re}}{\mathrm{Re} + hm}\sin\left(a\chi\right) \tag{9}$$

Where Re = Mean earth radius, 6371 km, *hm* = maximum height of electron density, 450 km, a = correction factor, 0.9782, χ = zenith angle and χ' = (90°- χ)

2.0 METHODOLOGY

The GPS receiver data analyzed in this study are obtained from GPS Malaysia. Malaysia has established two GPS networks that partly serve the purpose of geodetic survey, namely Malaysia Active GPS System (MASS) and the Malaysia Real-Time Kinematic Network System (MyRTKnet). MASS consist of 18 (10 in Peninsular) permenant GPS stations while MyRTKnet is a network of 27 (25 in Peninsular) continuous GPS stations. RTK survey method is the latest innovation of relative positioning whereby multiple receivers are linked by radios simultaneously in collecting observations. The present coverage of MyRTKnet includes three dense networks that provide centrimetre accuracy around Lembah Klang, Pulau Pinang and Johor Bahru and a sparse network covering the whole nation [13]. The data taken from receiver station located at Universiti Utara Malaysia, Kedah (Latitude (E) 06^0 Longitude (N) 100^0) and Sungai Petani, Kedah. (Latitude (E) 05 ^{0} Longitude (N) 100^0).

Fig.4. GPS stations of MyRTKnet

Fig.5. Two GPS stations of MyRTKnet UUMK and SGPT are used to study EPBs at low altitudes.

GPS signals at every 15 seconds are processed using scientific software. TEC along a ray path from the GPS satellite to the receiver is obtained by phase-averaging process on the pseudoranges. The GPSTk software from Applied Research Laboratories University of Texas, Austin was used as the processing software to process data from MyRTKnet. GPSTk is open source software, providing a core library and collection of applications that support GPS research, analysis and development. The code is released under the terms of the Lesser GNU Public License. TEC is processed by GPSTk assumption that the ionosphere consists of a thin shell at a fixed height, usually 350 or 400 kilometres, surrounding the Earth (single layer model, SLM) [14]. The GPS measurement of ionospheric TEC is complicated by the fact that hardware delays exist in both satellite and receiver. GPSTk performs data editing and computes TEC for RINEX format data files from the MyRTKnet site.

The GPSTk application process to obtain TEC is illustrated in Figure 7. It includes preprocessing for cycle slip detection and removal using DiscFix. Function application ResCor which generates slant TEC and removal satellite biases. The TEC variations can be conveniently classified in terms of regular and irregular variations. Regular variations represent the low frequency, long term trend of TEC, while the irregular variations contain the high frequency, short term part. EPBs effects cause dropness of frequency changes in the TEC. Taking advantage of this phenomenon, the method developed here detects the existence of EPBs by identifying dropness frequency changes in the VTEC values. To do this, the method assumes that VTEC data corresponding to satellite-to-ground station paths are time series in the universal time (UT) and de-trending data from diurnal variations and elevation angle dependences.

In this project, the trend of the original vertical TEC series for one satellite pass is obtained by calculating the average values within a moving window. The third order is the 1 hour window of Savitzky-Golay technique that was chosen. An elevation cut-off 40° was used to avoid effects of elevation angle dependencies such as multipath. Then the statistical analysis of the daily ΔTECv variation was constructed by using Matlab in order to identify possible the present of EPBs.

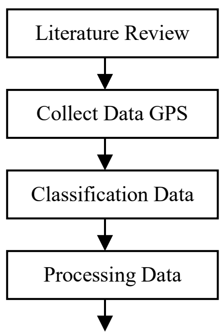

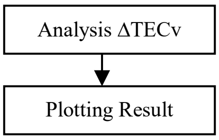

Fig.6. General Flowchart process of project

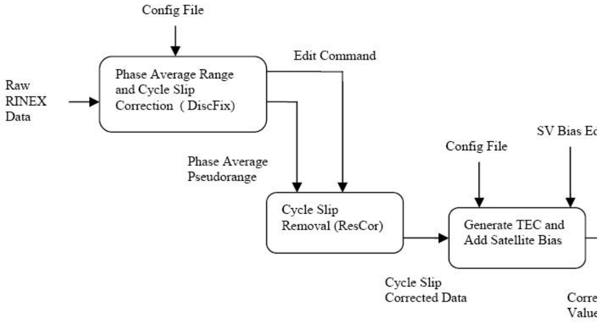

Fig.7. GPSTk TEC data processing [Gaussiran (2004)]

3.0 RESULTS

The results of the observed ΔTECv presented in this section. For the result of occurrence of plasma bubble, the data been chosen from Local Time Clock, LTC 02:00am – 04:00am (Universal Time Clock (UTC) 18:00 to 20:00). This is because the amount of plasma bubble occurred on night time much more than other. Figure 8a and b provides the vertical TEC all visible satellite (over 25 satellites) obtained at two stations MyRTKnet; SGPT and UUMK at 6th September 2007. From this figure show that VTEC hourly variation over two stations have small different between stations, but found the negative TEC. These negative TEC occur because of the receiver bias. The measurement of Ionospheric TEC is complicated because of delay where exist in both satellite and receiver. However, because this project focuses on Equatorial Plasma Bubbles (EPBs), so we only need to study the relatives' changes in TEC.

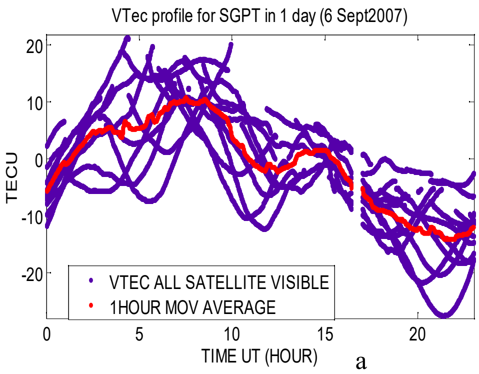

a

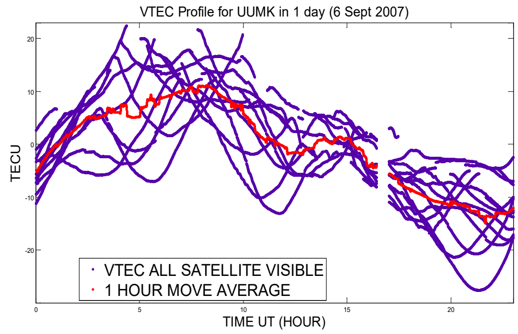

b

Fig.8a & b refer to VTEC all satellites in one day.

The red line represents the smoothing line for one day at GPS station. There are cut off at around hour 17.00 UT because the receiver could not get the data on that day. The blue line represents the data for all satellite in one day. Figure 9 present an example of plasma-bubble events which occurred over equatorial and low-latitude regions in SGPT and UUMK station during the magnetic storm of 6th September 2007. While figure 10 present the TEC depletion or plasma bubble at LTC around 2.00am

.

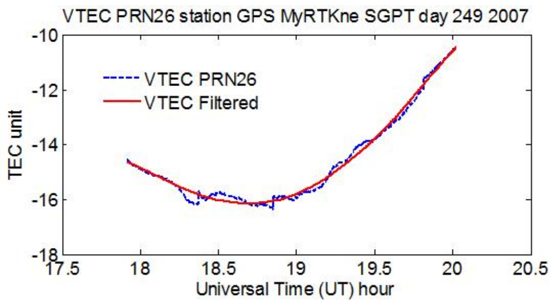

a

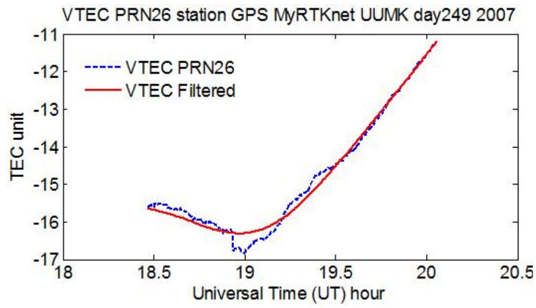

b

Fig.9a & b refer to occurrence of Plasma Bubbles at reference's station

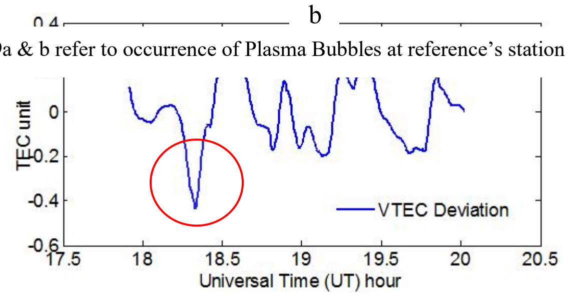

a

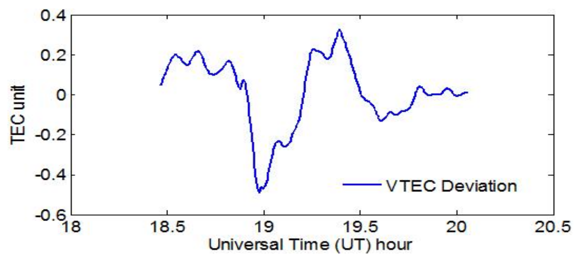

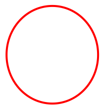

b

Fig.10a & b refer to occurrence of Plasma Bubbles

Figure 11a is reading for TECv which being recorded without the occurrence of plasma bubble for ARAU and figure 12b is reading for TECv which being recorded without the occurrence of plasma bubble for AYER. Both graphs are reading which being observed for one day, where on 3rd September 2007 for all satellites in Peninsular Malaysia (over 25 satellites)

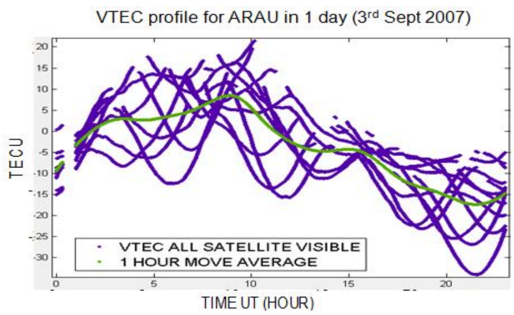

a

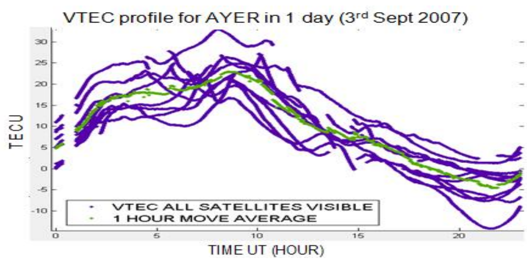

b

Figure11a & b: VTEC all satellites in 1 day

The green line represents the smoothing line for one day with one hour moving average as reference at GPS station. There are cut off at around hour 01.00 UT because the GPS receiver maybe could not get the data on that day. The blue line represents the data for all satellite in one day.

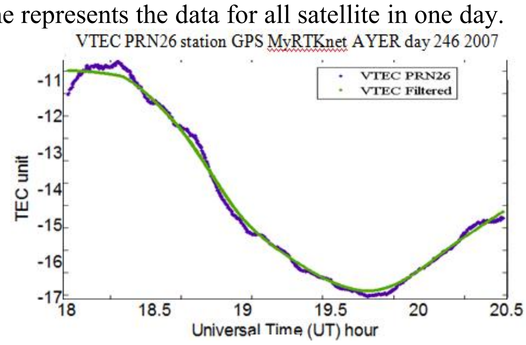

a

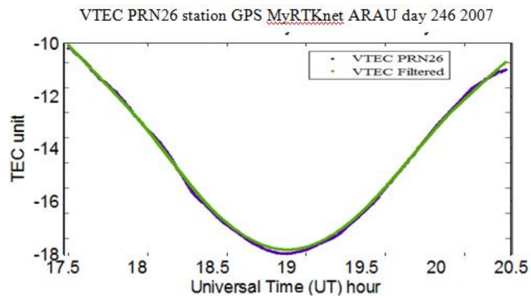

b

Figure 12a & b: non-occurrence of Plasma Bubbles

The days that have no EPBs likes 3rd September 2007, the sun activity is inactive where there is no effect occurred to the earth magnetic field [15]. Ionization process was reduced and the intensity of TEC also less, so that ΔTEC not show large changes. Therefore the amount of existing of EPBs is small. Figure 12(a) and (b) show that no irregularities or an extra unordinary depletion occurs detects on that day at AYER and ARAU station.

The universal time distribution of the first occurrence of the plasma-bubble events, and duration distribution at equatorial and low latitudes are plotted in Fig.10a and b, where was have red circle respectively. They display that most equatorial plasma bubbles start occur at 18:00 UT, and may last for less than 60 min. However, the dependence of the first occurrence of low latitude plasma bubbles on local time is at its maximum at 20:00 UT, and most plasma bubble events last for less than 45 min. It indicates that the duration of plasma bubbles becomes greater as one approaches the equator (Chandra, 1993; Singh, 2004).

Taking into account that most plasma-bubble events commence at pre-midnight, and the sample for post-midnight is not enough to perform a statistical analysis, especially for equatorial regions, in this paper we limit our attention to the dependence of plasma bubble occurrence for two stations on day 249 in the pre-midnight sector (18:00– 20:00 UT). The days that have no EPBs likes 18th September 2007, the sun activity is inactive where there is no effect occurred to the earth magnetic field [16]. Ionization process was reduced and the intensity of TEC also less, so that ΔTEC not show large changes. Therefore the amount of existing of EPBs is small. It is different to the day that has EPBs on 6th September 2007; start with the impact of CME (coronal mass ejections) to the magnetic field, solar flares and solar wind will compress magnetic field.

4.0 DISCUSSION

In this paper, we have Huang (2001) have also reported the maximum occurrence of EPBs were in equinoctial months (March, April, September and October) than the other months of 2007. Huang (2001) also obtained maximum rate of EPB occurrence in the equinox, least in the summer and moderate in winter. That is other reason where we can find that the EPB occur majorly in March and September. In this project we are focus in September only. The days that have no EPBs likes 3rd September 2007, the sun activity is inactive where there is no effect occurred to the earth magnetic field [17]. Ionization process was reduced and the intensity of TEC also less, so that ΔTEC not show large changes. Therefore the amount of existing of EPBs is small. It is different to the day that has Plasma Bubble on 6th September 2007; start with the impact of CME (coronal mass ejections) to the magnetic field, solar flares and solar wind will compress magnetic field. The solar wind pressure on the magnetosphere will increase or decrease depending on the Sun's activity. These solar wind pressure changes modify the electric currents in the ionosphere. Thus, increasing of electric field will produce many disturbances in form of gravity waves that refer to Equatorial Plasma Bubbles.

5.0 CONCLUSION

In this project we present the time and reason occurrence of Equatorial Plasma Bubbles (EPBs). Detection and analysis of occurrence of TEC is studied by using MyRTKnet GPS Network Malaysia. Data are evaluated on day 249 only from two stations. From analysis obtained, it is possible to detect the presence of Equatorial Plasma Bubbles every day. A few steps further should be taken to study more details about this topic. Taken data from many different stations, different sources such as Radar and ionosonde and analysis more PRN satellites; this will give the results more accurate in process obtaining EPBs.

REFERENCES

[1] MichiNishioka (nishioka@kugi.kyoto-u.ac.jp) Plasma bubble in the ionosphere, Department of Geophysics, Kyoto University

[2] G.Li, BNin, L.Liu, W.Wan and J.Y.Liu," Effect of magnetic activity on plasma bubbles over equatorial and low –latitude regions in East Asia" 1Beijing National Observatory of Space Environment, Institute of Geology and Geophysics, Chinese Academy of Sciences, Beijing, China, 2Institute of Space Science, National Central University, Chung-Li, Taiwan: 19 January 2009

[3] Ionosphere, available: http://www.en.wikipedia.org/wiki/Ionosphere#measurements/

[4] .Dimitar Ouzounov, Friedemann T. Freund, "Ground-Atmosphere-Ionosphere Interactions Related to Earthquake", NASA Goddard Space Flight Center/SSAI, Mailstop 902, Greenbelt, pp. 2-5. *ouzounov@eosdata.gsfc.nasa.gov*

[5] Geomagnetic Storm, (July 2007), available: *http://en.wikipedia.org/wiki/Geomagnetic_strom*

[6] Electron Content from GPS, (July 2007), available: *http://www.gpsworld.com/gpsworld/article/*

[7] J. Y. Liu1, Y. J. Chuo, S. J. Shan, Y. B. Tsai, Y. I. Chen, S. A. Pulinets, and S. B. Yu, "Pre-earthquake Ionospheric Anomalies Registered by Continuous GPS TEC Measurements", Annales Geophysicae, 2004, p.p 1588-1589

[8] Mohamad Huzaimy Jusoh, Norsuzila Ya'acob, Mardina Abdullah, Mahamod Ismail, "Signal Propagation Effects: Comparison of Total Electron Content (TEC) using Real Time Kinematic (RTK) Data during Quiet and Disturbed day at the Equatorial Ionosphere",

[9] Kyriaky Eftaxiadis, Dr Manuel A. Cervera, Dr Richard M. Thomas, "A Global Positioning System Receiver for Monitoring Ionospheric Total Electron Content", Surveillance Systems Division Electronics and Surveillance Research Laboratory, pp. 3-7

[10] Kyriaky Eftaxiadis, Dr Manuel A. Cervera, Dr Richard M. Thomas, "A Global Positioning System Receiver for Monitoring Ionospheric Total Electron Content", Surveillance Systems Division Electronics and Surveillance Research Laboratory, pp. 3-7.

[11] Asnawi, Mardina Abdullah, M.A Momani, "Analysis Of TEC Variation With The Occurrence Of Medium Scale Travelling Ionospheric Disturbance (MSTID)",

[12] Andrzej Krankowski, Irina E.Zakharenkova, Irk I. Shagimuratov, "Response of the ionosphere to the Baltic Sea earthquake of 21 September 2004",

[13] JUPEM 'Malaysian RTK GPS Networks (MyRTKnet) Guideline' *http://www.gpsworld.com/gpsworld/article/*

[14] The GPSTk home page, hosted by SourceForge.net http://www.gpstk.org/

[15] Dimitar Ouzounov, Friedemann T. Freund, "Ground-Atmosphere-Ionosphere Interactions Related to Earthquake", NASA Goddard Space Flight Center/SSAI, Mailstop 902, Greenbelt, pp. 2-5. *ouzounov@eosdata.gsfc.nasa.gov*

[16] J. Y. Liu1, Y. J. Chuo, S. J. Shan, Y. B. Tsai, Y. I. Chen, S. A. Pulinets, and S. B. Yu, "Pre-earthquake Ionospheric Anomalies Registered by Continuous GPS TEC Measurements", Annales Geophysicae, 2004, p.p 1588-1589

[17] Dimitar Ouzounov, Friedemann T. Freund, "Ground-Atmosphere-Ionosphere Interactions Related to Earthquake", NASA Goddard Space Flight Center/SSAI, Mailstop 902, Greenbelt, pp. 2-5. *ouzounov@eosdata.gsfc.nasa.gov*